



ChemComm

Chemical Activation of Commodity Plastics for Patterned Electroless Deposition of Robust Metallic Films

Journal:	<i>ChemComm</i>
Manuscript ID	CC-COM-07-2022-003848.R1
Article Type:	Communication

SCHOLARONE™
Manuscripts

COMMUNICATION

Chemical Activation of Commodity Plastics for Patterned Electroless Deposition of Robust Metallic Films

Jessica R. Wagner,^a Jared Fletcher,^a and Stephen A. Morin^{*a,b,c}Received 00th January 20xx,
Accepted 00th January 20xx

DOI: 10.1039/x0xx00000x

A general approach to increase the adhesion of metal films to commodity plastic substrates using a metal-chelating polymer, polyethyleneimine, in conjunction with patterned electroless deposition is described. This general fabrication method is compatible with a diverse array of plastics and metals with properties applicable to flexible electronic circuits and electrochemical cells.

A general, low-cost procedure for the patterned deposition of a range of metals onto flexible polymeric substrates would be useful to many technologies including, for example, flexible electronics, sensors, and displays.¹ Existing procedures, such as the lithographic fabrication of printed circuit boards (PCBs), are optimized for the deposition of a specific metal (e.g., copper) on planar surfaces and require multiple steps (e.g., masking, etching, etc.).² Patterned electroless deposition of metals can offer a simple and cost-effective alternative to these procedures, but metallic traces created using electroless deposition are prone to delamination due to weak adhesion even when etching procedures are used to prepare the surface.³ We desired a general procedure for the electroless deposition of well-adhered metal films onto a range of commodity plastics.

We developed a method to functionalize the surface of commodity plastics with a metal chelating polymer (polyethyleneimine) which ligates metal cations and promotes the formation/adhesion of seed particles during the initial activation step of electroless deposition. When coupled with reconfigurable/resealable microfluidic devices and bulk bath

deposition procedures, patterned and/or homogeneous metallic films with strong adhesion supportive of several applications were readily accessible. We demonstrated the compatibility of this process with serial depositions for the fabrication of patterned traces of different metals. We illustrated the functionality of the metallic traces in prototypical electronic and electrochemical applications.

The reported method, which we term microfluidic directed metal deposition (μ DMD), is applicable to several functional metals (copper, silver, nickel, and gold) and a range of polymeric substrates (polycarbonate, polyethylene, etc.). μ DMD provides fabrication capabilities useful to the manufacturing of flexible electronic systems, including sensors and displays, point-of-care devices, and electrochemical probes. The increased mechanical stability of the traces generated using μ DMD makes it a viable fabrication option for generating wearable/flexible electronics, smart packaging, etc.

Traditional methods for the manufacture of printed circuit boards (PCBs) can be additive or subtractive and typically use photolithography to designate the pattern. In a typical workflow, patterned photoresist is used to mask bare or metal-coated polymeric supports enabling patterned deposition of desired metals or selective etching, respectively, to yield conductive metallic traces.^{1b} Disadvantages of these methods include lengthy processing and post-processing steps, especially when multiple metals are required, incompatibility with non-planar substrates, and costly material waste.⁴ For these reasons, other methods to generate patterned metallic traces have been explored, such as direct printing, screen printing, laser-direct structuring, electrolytic deposition, vapor deposition, and electroless deposition.^{2, 5} We focused on electroless deposition due to its many advantages. Specifically, electroless deposition is operationally simple, requiring few steps and a minimal amount of equipment and materials, and it works at low temperatures, making it ideal for low-cost, scalable manufacturing.⁶ Electroless deposition uses a chemical reducing agent to deposit metals at designated sites, thus eliminating the need for external power supplies.⁷ The location

^a Dept. of Chemistry, University of Nebraska–Lincoln, Hamilton Hall, Lincoln, NE 68588.

^b Nebraska Center for Materials and Nanoscience, University of Nebraska–Lincoln, Lincoln, NE 68588.

^c Nebraska Center for Integrated Biomolecular Communication, University of Nebraska, Lincoln, Lincoln NE 68588.

* To whom correspondence should be addressed. Telephone: (402) 472-4608. Fax: (402) 472-9402. E-mail: smorin2@unl.edu.

Electronic Supplementary Information (ESI) available. See DOI: 10.1039/x0xx00000x

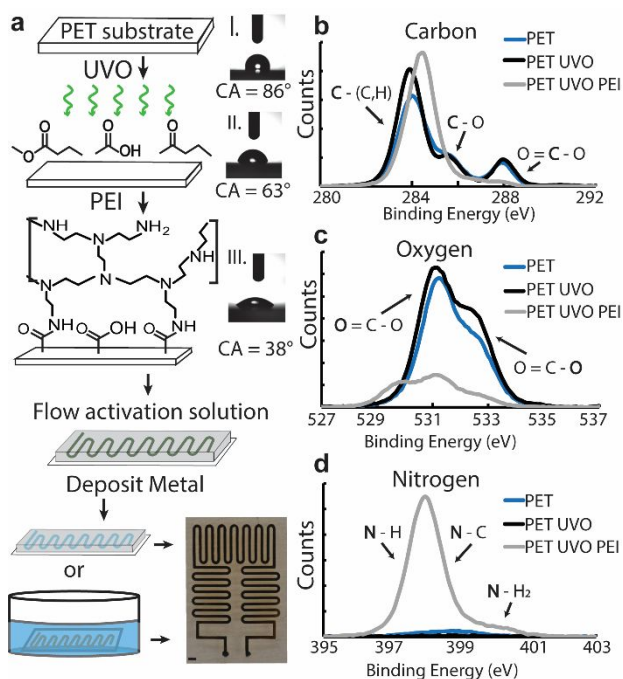


Fig. 1 Microfluidic-directed metal deposition (μ DMD) on PEI modified plastics. (a) Schematic illustration of the chemical modification of polymer substrates with PEI and subsequent μ DMD. A representative image of gold on PET is included (scale bar is 1.5 mm). Static water contact angle data of a PET substrate before modification (I), after UVO treatment (II), and after PEI treatment (III) is given as insets. (b-d) XPS data of a PET substrate throughout surface modification.

of deposition is controlled by activating portions of the target surface with seed particles (e.g., tin and palladium) that promote the electroless reduction/deposition of the target metal. While effective at controlling the deposition process, the adhesion of the seed particles to polymeric materials is weak, and metal delamination remains a significant problem.⁸

Topographic and chemical surface modifications have been used to improve the adhesion of metals deposited using electroless protocols. Introducing topography or micro-roughness onto surfaces, through chemical etching for example, increases surface area and by extension seed particle adhesion.^{7a} This process increases the ability of the metallic films to withstand mechanical abrasion; however, they can nevertheless be peeled during contact tests (e.g., tape tests). In addition, the need for harsh chemical etchants (e.g., strong oxidizers and alkali solutions) makes this method undesirable.

Different polymers have been used as chemical adhesion promoters in polymer-assisted electroless deposition methods.^{1a, 9} However, these methods are dependent not only on the surface-polymer interaction, but the interaction of the polymer and seed particles as well. Therefore, it can be difficult to develop a general method that works for a variety of different substrate materials and metals. Metal-chelating polymers, such as polyethyleneimine (PEI), are of interest due to their ability to bind to a variety of metal particles.¹⁰ PEI contains branched amine groups which are known for their strong affinity towards metal cations due to their Lewis base character. While PEI has been used to generate biofunctional coatings and tune nanoparticle surfaces, its use in the electroless deposition of metals has yet to be explored.¹¹

We hypothesized that by covalently attaching PEI to target substrates, the metal seed particles required for electroless

deposition would be effectively adhered to the substrate through the formation of strong coordination bonds with the surface-bound chelating polymer. Commodity plastics are, however, generally incompatible with common surface conjugation reactions, and the surfaces would require surface-chemical activation. It has been shown that ultra-violet ozone (UVO) can be used to oxidize the surface of commodity plastics creating surface carboxylic acids, esters, and ketones.¹² These carbonyl moieties allow for further functionalization of the plastics through different conjugation schemes. In the case of PEI, the primary amines of the polymer network can form amide bonds through nucleophilic attack of surface carboxylates.^{12a, 13}

The ability to pattern where the electroless deposition of metals occurs is essential for generating conductive traces for electronic circuits. Traditionally, microfluidic devices are permanently bonded to their underlying substrates.¹⁴ While this characteristic is critical to lab-on-a-chip applications in sensing, chemical screening, etc.,¹⁵ it is generally not useful to derivatizing surfaces with microfluidic reactors. We previously demonstrated the design and operation of resealable microfluidic devices and reported the use of these devices in the patterned electroless deposition of copper on 3-dimensional substrates. Etchant-induced microroughness was the mode used to promote adhesion, but we observed extremely weak adherence of the deposited copper.¹⁶ Here we overcome this persistent problem in electroless deposited metals by using the concept of metal chelating PEI discussed above in conjunction with resealable microfluidic devices.

We demonstrated our approach using a representative set of commodity plastics, polycarbonate (PC), polyethylene terephthalate (PET), polypropylene (PP), polyvinyl chloride (PVC), acrylonitrile butadiene styrene (ABS), and functional metals (copper, silver, nickel, and gold). Together they demonstrate the versatility of our procedure across the repertoire of polymers and metals used in reel-to-reel manufacturing. UVO is used as a convenient and scalable method to oxidize the polymeric substrates. In addition, using UVO eliminates the need for a harsh chemical etching step, is a quicker process, and can be patterned if necessary. X-ray photoelectron spectroscopy (XPS) is an ideal method for analyzing the surface chemistry of a material, therefore we used it to track the change in chemical speciation of our surfaces throughout functionalization. We used PET as a representative XPS study case for the surface modification because its oxidation with UVO is well documented.¹⁷

Surface treatment with UVO and PEI led to strong adhesion of deposited traces of copper, nickel, silver, and gold that was stronger than on untreated surfaces (Fig. 1a, S1, S12, S13). The UVO oxidizes the substrates creating different carbonyl functional groups (carboxylic acids, esters, ketones) on the surface. The primary amines in the PEI then form amide bonds with the carbonyls on the polymeric surface, rendering the surface functionalized with free amine groups (Fig. 1a). We used XPS to monitor the stepwise surface modification of a PET substrate through UVO and PEI treatment. We observed a large peak at 284 eV in the carbon spectra which corresponds to the C-C/C-H bond. The smaller peaks near 285 and 288 eV were

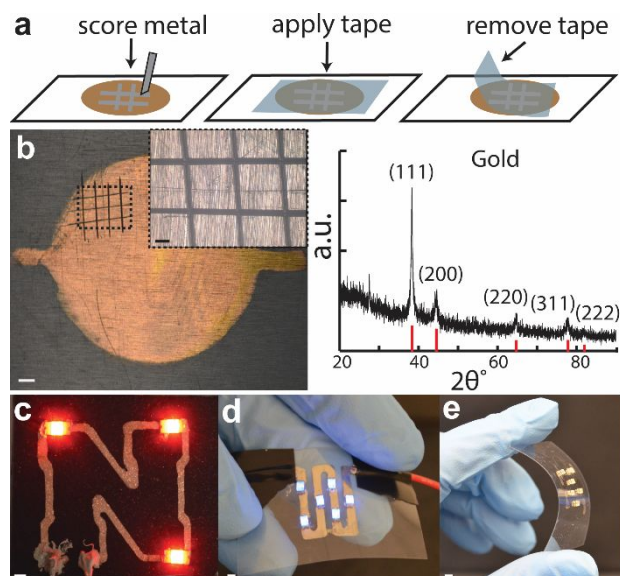


Fig. 2 (a) Schematic illustration of the tape test. (b) Representative optical micrographs of μ DMD gold after the tape test. The annotated test region is given as high magnification inset (left). Representative XRD data with each primary peak indexed (right) (PDF no. 04-0784). (c-e) Representative μ DMD traces used to power surface-mount LEDs. Inset scale bars are 250 μ m, all others are 1.5mm.

signals from the carbon-oxygen bonds (Fig. 1b). We observed an increase in the signal of the oxygen 1s peaks after treatment with UVO, due to the increase of oxygen rich functional groups on the surface (e.g., carbonyls and esters). The main two peaks in the oxygen spectra, near 531 and 533 eV, correspond to the different oxygen-carbon bonds (Fig. 1c). Following PEI treatment, we observed a decrease in the oxygen content on the surface, which can be seen in the signals of both the carbon and oxygen spectra. After functionalization with PEI, we observed a shift in the primary carbon (C-C) peak towards \sim 285 eV, due to the formation of amide bonds. A corresponding decrease in the intensity of the -COO peak at 289 eV was consistent with a loss of carbonyl groups during amide bond formation. Emergence of a nitrogen peak at 398 eV also indicated successful PEI modification (Fig. 1b-d).

In parallel, we monitored the change in surface chemistry using static water contact angle measurements. Treatment with UVO caused a decrease in the contact angle of PET from 86° to 63°, and attachment of PEI caused the contact angle to further decrease to 38°. The increase in hydrophilicity can be attributed to the increased polar interactions of water with the oxidized surfaces and nitrogen rich PEI, respectively (Fig. 1a). The contact angle and XPS data, which together reflected significant changes to surface wettability and chemical speciation, supported our conclusion that PEI was reliably attached to the PET substrates modified using this simple procedure.

We replicated the above functionalization procedure on commodity plastics PVC, PP, and ABS, with the exception of PC, which is extremely susceptible to UV degradation due to photo-Fries rearrangement and photooxidation.¹⁸ In the case of PC, the UVO activation was omitted and the native polymer chemistry was enough to support the functionalization with PEI through urethane bonds (Fig. S3, S4).¹⁹ Due to their metal-chelating nature, the amine groups in PEI act as ligands towards the tin and palladium seed particles in the activation solution.

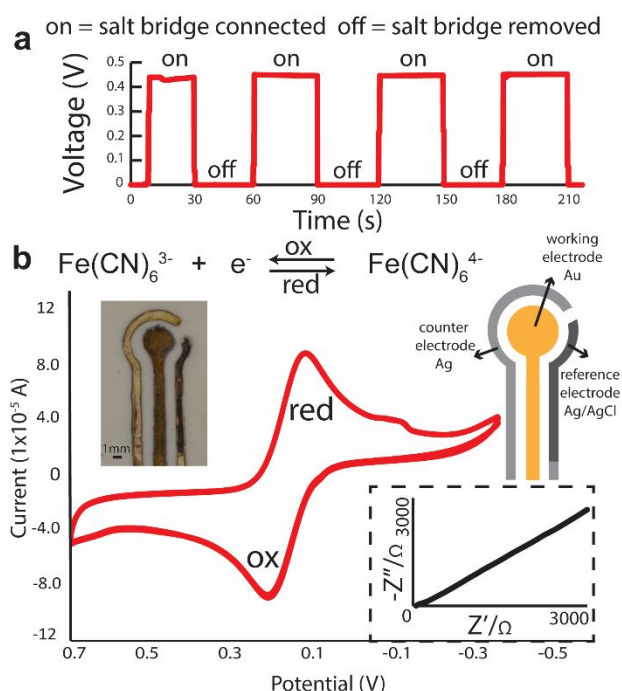


Fig. 3 Electrochemical applications of multi-metal μ DMD patterns. (a) Temporal voltage output of the galvanic cell. The half-cells are connected and disconnected using a salt bridge. (b) Schematic and representative optical micrograph of three microelectrodes used to construct and operate a voltametric cell. The working electrode (gold), counter electrode (silver), and reference electrode (silver/silver chloride) were deposited onto ABS substrate. Representative cyclic voltammogram of ferricyanide/ferrocyanide measured using the μ DMD microelectrodes. (Inset) electrical impedance spectroscopy of gold electrode.

The Sn^{2+} particles reduce the Pd^{2+} particles to Pd in situ, which act as a site for the electroless metal deposition to occur. After deposition, the deposition only occurred in the areas activated through the microfluidic devices (Fig. S1).

X-ray diffraction patterns were collected and used to confirm the identity/crystallinity of the deposited metal films/traces. In the diffractograms of each metal (copper, nickel, silver, and gold), the primary peaks match those expected (Fig. 2b, S5). Further, the representative diffractograms of the deposited copper, silver, and gold films indicated a polycrystalline morphology consistent with other reports of electroless deposition. In the case of nickel, we observed a broad peak centered around 45° which was consistent with other reports of electroless deposition of nickel (Fig. S5c).²⁰

To test the adhesion strength, we scored the deposited traces, and a tape test was performed. Microscope images were taken after removal of the tape and we observed no peeling of any of the metals, demonstrating excellent adhesion to the optimally functionalized substrates which surpassed the cohesive strength of the films themselves (Fig. 2a,b, S2, S5, S6, S13). To demonstrate the conductivity of the deposited metals, they were used as conductive traces to power surface mount LEDs. The LEDs lit up when voltage was applied to the circuits, illustrating the conductivity of the deposited metals (Fig. 2c-d). The excellent adhesion of the produced metallic traces enabled mechanical deformation of the substrate without delamination or loss of conductivity (Fig. 2d-e). After 100 bending cycles ($r=10$ mm), we observed no change in the electronic performance nor cracking/peeling of the trace (Fig. S7, S8). We observed virtually no change in resistance through a bending cycle (Fig. S9).

The deposited metals can also be used as electrodes in electrochemical applications. To demonstrate this, we fabricated a simple battery cell using copper and silver as the electrodes, deposited on PP substrates (Fig. S10). We connected the “half-cells” with a salt bridge, which could be removed and added to turn the battery “off” and “on”. The voltage produced from the battery in the “on” state was 0.45 V (Fig. 3a) consistent with the voltage calculated using standard reduction potentials and the Nernst equation. We also fabricated an integrated electrochemical cell using patterned microelectrodes. Specifically, we deposited gold (working), silver (counter), and silver/silver chloride (reference) microelectrodes on ABS substrates (Fig. 3b). To generate the reference microelectrode, the top layer of a silver trace was converted into silver chloride (see ESI). After conversion of the silver trace to silver chloride the primary peaks produced from XRD matched with the expected peaks of silver chloride, confirming successful transformation (Fig. S11). We then tested the operation of the microelectrode system in electrochemical analysis by interrogating the ferricyanide/ferrocyanide redox using cyclic voltammetry (CV). We observed a cathodic peak, indicative of the reduction of ferricyanide to ferrocyanide, at around 0.1 V and an anodic peak, indicative of the reverse oxidation process, around 0.2V, consistent with the expected peaks for the ferricyanide/ferrocyanide redox couple (Fig. 3b).²¹ We attributed the small peak near -0.1V due to the PEI on the surface in between the electrodes. We performed electrochemical impedance spectroscopy (EIS) and near ideal behavior of the gold electrode was observed (Fig. 3b).

We developed a general procedure to functionalize the surface of various flexible polymeric substrates with the metal chelating polymer PEI, which acts as an excellent adhesion promoter during the electroless deposition of a range of metal traces. We demonstrated the durability of these traces using adhesion tests and mechanical deformations and illustrated the functionality of these metals in simple electronic circuits and electrochemical devices. The method we report is quick, low-cost, and simple to execute using benign aqueous chemistry, providing numerous advantages over traditional PCB fabrication methods. The procedures we report are readily applicable to 3D substrates and intricate multi-metal designs useful to, for example, molded interconnects and 3D antennas. We believe μ DMD represents a potentially transformative approach to the low-cost, scalable fabrication of flexible circuits, sensors, and wearables using electroless protocols. In the future μ DMD can be combined with the bath deposition of insulators and semiconductors to realize a greater diversity of material combinations and their associated applications.

We thank Prof. Lai's group at UNL for help with CV and EIS experiments. This work was supported by the National Science Foundation under grant DMR-1555356. This research was performed in part at the Nebraska Nanoscale Facility: National Nanotechnology Coordinated Infrastructure and NCMN, which are supported by the National Science Foundation under Award ECCS: 1542182, and the Nebraska Research Initiative.

There are no conflicts to declare.

Notes and references

- a) F. T. Zhang, L. Xu, J. H. Chen, B. Zhao, X. Z. Fu, R. Sun, Q. W. Chen and C. P. Wong, *ACS Appl. Mater. Interfaces*, 2018, **10**, 2075-2082; b) H. Shamkhalichenar, C. J. Bueche and J.-W. Choi, *Biosensors*, 2020, **10**, 159; c) T. H. Phung, J. Jeong, A. N. Gafurov, I. Kim, S. Y. Kim, H.-J. Chung, Y. Kim, H.-J. Kim, K. M. Kim and T.-M. Lee, *Flex. Print. Electron.*, 2021, **6**, 024001.
- S. M. Mirvakili, K. Broderick and R. S. Langer, *ACS Appl. Mater. Interfaces*, 2019, **11**, 35376-35381.
- J. K. Pancracious, S. B. Ulaeto, R. Ramya, T. P. D. Rajan and B. C. Pai, *Int. Mater. Rev.*, 2018, **63**, 488-512.
- D. Zabetakis and W. J. Dressick, *ACS Appl. Mater. Interfaces*, 2009, **1**, 4-25.
- a) C. T. Wan, K. A. Taylor, D. L. Chambers and G. T. Susi, in *Metallized Plastics 2*, Springer US, 1991, 6, pp. 81-95; b) K. Clay, I. Gardner, E. Bresler, M. Seal and S. Speakman, *Circuit World*, 2002, **28**, 24-31; c) J. G. V. Scott, *Circuit World*, 2005, **31**, 34-41; d) A. Eshkeiti, A. S. G. Reddy, S. Emamian, B. B. Narakathu, M. Joyce, M. Joyce, P. D. Fleming, B. J. Bazuin and M. Z. Atashbar, *IEEE Trans. Compon. Packaging Manuf. Technol.*, 2015, **5**, 415-421; e) A. Alwaidh, M. Sharp and P. French, *Opt. Lasers Eng.*, 2014, **58**, 109-113; f) B. N. Smirnov, V. N. Kozhanov and V. N. Chuprakov, *Russ. J. Appl. Chem.*, 2001, **74**, 1821-1828; g) J. H. Lee, *Mater. Sci. Forum*, 2007, **544-545**, 709-712.
- Y. Shacham-Diamand, T. Osaka, Y. Okinaka, A. Sugiyama and V. Dubin, *Microelectron. Eng.*, 2015, **132**, 35-45.
- a) S. Ghosh, *Thin Solid Films*, 2019, **669**, 641-658; b) P. Bindra and J. Roldan, *J. Electrochem. Soc.*, 1985, **132**, 2581-2589.
- R. Bernasconi, G. Natale, M. Levi and L. Magagnin, *J. Electrochem. Soc.*, 2016, **163**, D526-D531.
- a) X. Liu, X. Zhou, Y. Li and Z. Zheng, *Asian J. Chem*, 2012, **7**, 862-870; b) P. Li, Y. K. Zhang and Z. J. Zheng, *Adv. Mater.*, 2019, **31**, 16.
- a) G. I. Dzhardimalieva and I. E. Uflyand, *J. Inorg. Organomet. Polym. Mater.*, 2018, **28**, 1305-1393; b) S. Kobayashi, K. Hiroishi, M. Tokunoh and T. Saegusa, *Macromolecules*, 1987, **20**, 1496-1500.
- a) M. Liu, J. Ji, X. Zhang, X. Zhang, B. Yang, F. Deng, Z. Li, K. Wang, Y. Yang and Y. Wei, *J. Mater. Chem. B*, 2015, **3**, 3476-3482; b) X. Wang, L. Zhou, Y. Ma, X. Li and H. Gu, *Nano Res.*, 2009, **2**, 365-372.
- a) J. M. Taylor, K. Perez-Toralla, R. Aispuro and S. A. Morin, *Adv. Mater.*, 2018, **30**, 8; b) J. Deng, L. Wang, L. Liu and W. Yang, *Prog. Polym. Sci.*, 2009, **34**, 156-193.
- G. A. Castillo, L. Wilson, K. Efimenko, M. D. Dickey, C. B. Gorman and J. Genzer, *ACS Appl. Mater. Interfaces*, 2016, **8**, 35641-35649.
- A. Borók, K. Laboda and A. Bonyár, *Biosensors*, 2021, **11**, 292.
- A.-G. Niculescu, C. Chircov, A. C. Bîrcă and A. M. Grumezescu, *Int. J. Mol. Sci.*, 2021, **22**.
- a) A. Konda, J. M. Taylor, M. A. Stoller and S. A. Morin, *Lab Chip*, 2015, **15**, 2009-2017; b) A. Konda, A. Rau, M. A. Stoller, J. M. Taylor, A. Salam, G. A. Pribil, C. Argyropoulos and S. A. Morin, *Adv. Funct. Mater.*, 2018, **28**, 9.
- C. Ton-That, D. O. H. Teare, P. A. Campbell and R. H. Bradley, *Surf. Sci.*, 1999, **433**, 278-282.
- a) S. Redjala, N. Aït Hocine, R. Ferhoum, M. Gratton, N. Poirot and S. Azem, *J. Fail. Anal. Prev.*, 2020, **20**, 1907-1916; b) D. O. H. Teare, C. Ton-That and R. H. Bradley, *Surf. Interface Anal.*, 2000, **29**, 276-283.
- P. Jankowski, D. Ogończyk, W. Lisowski and P. Garstecki, *Lab Chip*, 2012, **12**, 2580.
- H. Mu, J. Seok and R. Y. Lin, *J. Electrochem. Soc.*, 2003, **150**, C67.
- S. Bollo, C. Yáñez, J. Sturm, L. Núñez-Vergara, J.A. Squella, *Langmuir*, 2003, **19**, 3365-3370.